Turning Adversaries into Allies: Reversing Typographic Attacks for Multimodal E-Commerce Product Retrieval

Janet Jenq and Hongda Shen* {janet.jenq,hongda.shen}@pitchbook.com PitchBook USA

Abstract

Multimodal product retrieval systems in e-commerce platforms rely on effectively combining visual and textual signals to improve search relevance and user experience. However, vision-language models such as CLIP are vulnerable to typographic attacks, where misleading or irrelevant text embedded in images skews model predictions. In this work, we propose a novel method that reverses the logic of typographic attacks by rendering relevant textual content (e.g., titles, descriptions) directly onto product images to perform vision-text compression, thereby strengthening image-text alignment and boosting multimodal product retrieval performance. We evaluate our method on three vertical-specific e-commerce datasets (sneakers, handbags, and trading cards) using six state-of-the-art vision foundation models. Our experiments demonstrate consistent improvements in unimodal and multimodal retrieval accuracy across categories and model families. Our findings suggest that visually rendering product metadata is a simple yet effective enhancement for zero-shot multimodal retrieval in e-commerce applications.

Keywords

Multimodal Representation Learning, Vision-Text Compression, Product Search, Typographic Attacks

ACM Reference Format:

1 Introduction

In e-commerce platforms, buyers and sellers engage with product listings through visual and textual information by viewing images, reading titles and descriptions, or searching with imageand keyword-based queries [14, 21]. Multimodal product retrieval matches queries to relevant items by combining signals from image

Permission to make digital or hard copies of all or part of this work for personal or classroom use is granted without fee provided that copies are not made or distributed for profit or commercial advantage and that copies bear this notice and the full citation on the first page. Copyrights for components of this work owned by others than the author(s) must be honored. Abstracting with credit is permitted. To copy otherwise, or republish, to post on servers or to redistribute to lists, requires prior specific permission and/or a fee. Request permissions from permissions@acm.org.

CIKM '25, Seoul, Republic of Korea

© 2025 Copyright held by the owner/author(s). Publication rights licensed to ACM. ACM ISBN 978-1-4503-XXXX-X/25/11

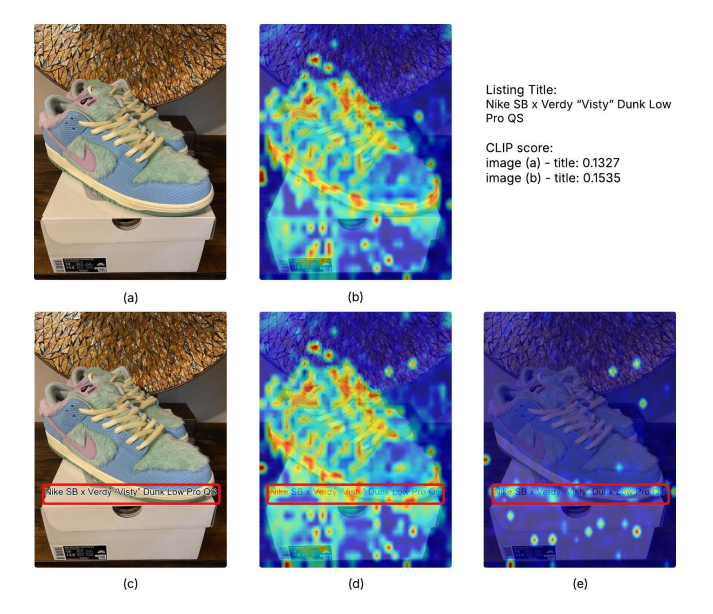


Figure 1: Visualization of the impact of title rendering on image representations, shown through changes in the attention sensitivity heatmap for the OpenAI CLIP ViT-Large model.

and text when either partial (e.g., only an image or a title) information or full (both image and title) information is available. By incorporating signals from both modalities, retrieval models can better capture user intent and improve result relevance. In practice, state-of-the-art models such as CLIP are widely adopted because their dual-encoder architecture, which encodes text and image inputs into a shared embedding space, allows efficient nearest-neighbor retrieval across unimodal and multimodal scenarios. The scalability and zero-shot generalization of these multimodal models make them particularly suited for large-scale e-commerce applications with vast search space and query diversity.

An emerging line of research has focused on understanding the impact of rendered visual text within images on the representations learned by contrastive vision-language models, particularly those in the CLIP family [7, 10, 12, 16, 18, 19]. Earlier studies [10, 12, 19] have demonstrated that overlaying irrelevant or misleading text on images can act as a form of adversarial attack against multimodal representation models. Specifically, these works introduce the notion of *typographic attacks*, in which visually rendered textual content manipulates model predictions by injecting misleading semantics. Large Vision-Language Models such as the CLIP family are trained on large-scale, weakly curated web data, where image

 $^{^{\}star}\text{Equal}$ contribution. Work performed while the authors were at eBay.

captions often describe visible elements rather than highlighting features that are most relevant for understanding the image. As a result, these models tend to attend to spurious correlations, which are patterns that emerge when visual and textual elements frequently appear together in the training data despite having no meaningful semantic relationship [19]. In a related but distinct line of work, CLIPPO [24] explores the possibility of building a unified representation for both image and text modalities by rendering text as image and processing both through a shared visual encoder. Their approach eliminates the need for modality-specific components, thereby simplifying the architecture and reducing the parameter count by approximately 50% compared to dual-encoder models such as CLIP.

Recently, DeepSeek-OCR [28] introduced a vision—text compression paradigm that renders textual content onto images, enabling visual encoders to absorb linguistic information and thereby unify vision and language representations for efficient OCR. Glyph [8], released shortly thereafter, generalized this concept to long-context modeling by rendering extended text sequences into visual forms processed by a VLM, achieving scalable context compression while maintaining semantic fidelity.

Motivated by these advances in vision-text compression, we propose a novel approach for enhancing multimodal product retrieval by reversing the logic of typographic attacks. Rather than injecting adversarial or misleading text, our method renders product-relevant information-such as titles, descriptions, and metadata-directly onto product images, thereby strengthening image-text alignment and improving retrieval performance. Unlike CLIPPO, which renders textual content into a separate image input, our approach embeds the text directly onto the original product image. This consolidation reduces the number of image inputs from two to one, reducing computational overhead during inference. An example of our method is shown in Figure 1, using the CLIP ViT-Large model. Subplot (a) shows a product image (Nike sneakers), and (c) shows the same image with the listing title rendered on top using our algorithm. Subplot (b) and (d) display attention sensitivity heatmaps generated using the method of Bousselham et al. [3] for the same text query applied to the raw and title-rendered images, respectively. The rendered title shifts attention toward the text region (highlighted by the red box), with Subplot (d) showing increased focus on semantic entities like "Nike" and "Verdy's Visty". In Subplot (e), we visualize the absolute difference between the two heatmaps, where changes are concentrated near the rendered title area. This attention shift suggests that title-rendered images yield embeddings more aligned with their textual counterparts, improving multimodal retrieval. In this example, the CLIP similarity score between the image and its title increases from 0.1328 (raw image) to 0.1535 (title-rendered image), indicating improved image-text alignment.

2 Related Work

Recent advances in vision-language pre-training demonstrate the effectiveness of integrating textual and visual information for e-commerce product retrieval applications [29, 31, 32]. In particular, Yu et al. [29] introduced *CommerceMM*, a multimodal representation learning framework capable of handling a wide range of

e-commerce tasks, including multimodal categorization, image-text retrieval, query-to-product retrieval, and image-to-product retrieval. To improve product matching in the fashion domain, Tóth et al. [25] proposed a model that integrates multiple image encoders and a single text encoder. However, the lack of open-source implementations and the domain-specific nature of these approaches restrict their utility in broader multimodal product retrieval settings.

CLIP [20] established a new paradigm in visual representation learning by employing natural language supervision. Building upon its success, several variants such as SigLIP [30] and SigLIP 2 [23] have been developed to further advance multimodal representation learning. Additionally, the Perception Encoder (PE) [2] family of vision encoders has achieved state-of-the-art performance across numerous vision tasks. By combining a robust contrastive pretraining objective with fine-tuning on synthetically aligned videos, PE models produce generalizable and scalable features for downstream tasks.

To the best of our knowledge, the term typographic attack was first introduced in Goh et al. [10] to describe a non-programmatic adversarial attack in which misleading or incorrect text is rendered directly onto an image to induce incorrect model predictions, particularly image classification tasks. Follow-up studies [1, 11, 12] have further investigated the mechanisms underlying typographic attacks and proposed various defense strategies. More recently, Oraitem et al. [19] extended the notion of typographic attacks to include non-matching text and graphical symbols, reflecting the prevalence of branding artifacts in web-scale training data. Although the root cause of such attacks remains underexplored, the prevailing view across the literature is that vision language models (VLMs), typically contrastive models like CLIP, are prone to learning spurious correlations, or unintended patterns arising from frequent but semantically unrelated co-occurrences [13, 26]. For instance, Lin et al. [13] observed that embedded text and corresponding image captions can introduce a strong text-spotting bias, which is intrinsic to the contrastive learning framework. To mitigate this effect, they proposed a data filtering approach based on OCR tools. Subsequent work has confirmed this bias and introduced alternative filtering strategies for CLIP training [4, 15, 27]. CLIP and SigLIP models are widely used as vision encoders in large multimodal models (LMMs), which combine vision-language models (VLMs) with large language models (LLMs) to support more advanced reasoning and interaction. Given the strong zero-shot performance of these encoders on tasks such as classification, retrieval, and segmentation, their sensitivity to typographic attacks is likely to propagate to LMMs as well [5, 6].

3 Methodology

3.1 Problem Formulation

We formulate multimodal product retrieval as the task of finding the most similar product given a query, where both the query and candidate products consist of an image and associated text. Given a query $q=(i_q,t_q)$, consisting of an image i_q and its associated text t_q , the objective is to retrieve the product $p=(i_p,t_p)$ that most closely matches the query from a candidate pool of e-commerce products \mathcal{P} . Image and text inputs are independently encoded by an image encoder and a text encoder, and the resulting features are fused into a joint multimodal embedding space f(i,t). Since

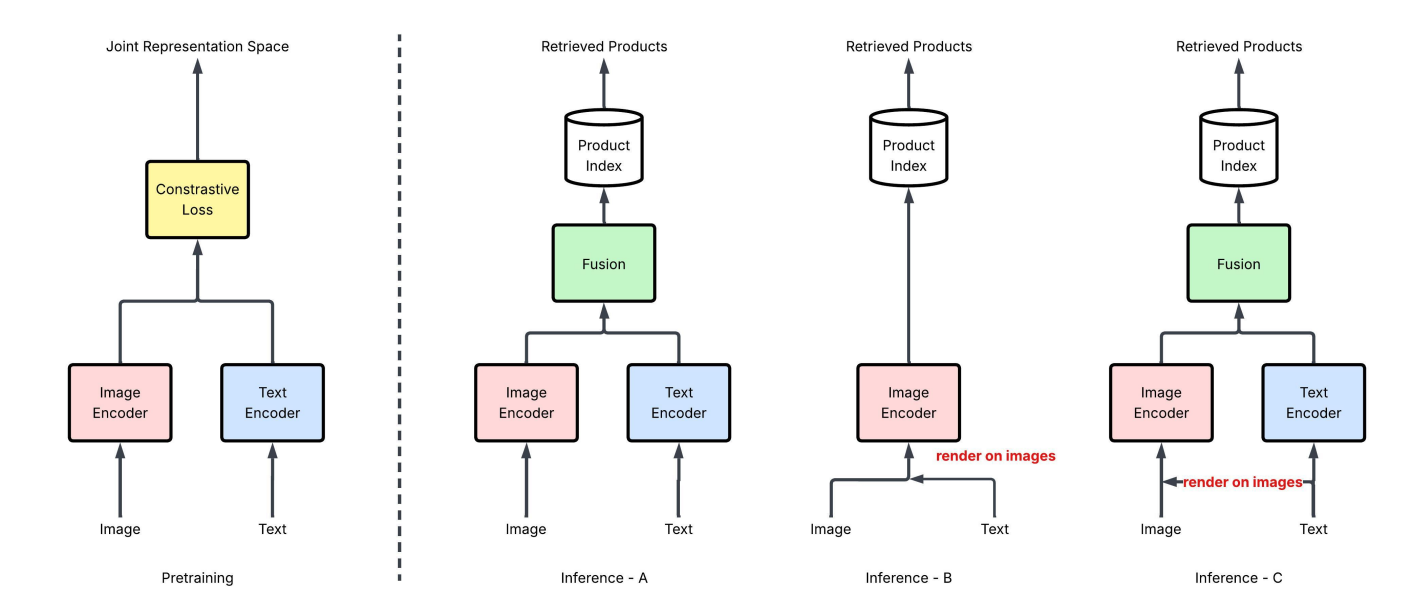


Figure 2: Overview of the proposed method, including two new inference modes that leverage text-rendered images for improved multimodal retrieval.

text inputs can be lengthy (e.g., item titles, product descriptions, and attribute lists), we leverage a Large Language Model (LLM) to summarize them, preventing excessive textual content from overshadowing the image. This summarization also facilitates alignment with text encoders, particularly when input token limits are imposed. For simplicity, we refer to the summarized text as the *title* throughout this paper, while noting that such inputs may originate from multiple sources within an e-commerce listing. The similarity between the query and a candidate item is computed using a similarity function $S(f(i_q,t_q),f(i_p,t_p))$, where we use cosine similarity throughout this work. The best-matching product is retrieved by ranking the similarity scores between the query and each candidate product. The left and right subplots in Figure 2 illustrate the training procedure and the inference-time flow, respectively.

3.2 Our Method

Typographic attacks leverage unintended correlations between semantic concepts and unrelated visual signals to manipulate the representations learned via contrastive models such as CLIP. Instead of the misleading text, the proposed approach reverses it to render product metadata on the image to strengthen image-visual text correlation which improves the product retrieval performance.

Figure 2 presents an overview of our method. The left subplot shows the pretraining stage, where a joint image-text embedding space is learned via contrastive learning. In zero-shot settings, models are trained on large-scale, weakly curated web data. These models can optionally be fine-tuned on domain-specific datasets when sufficient data is available.

The right subplot depicts three inference pathways for generating query and index embeddings. These embeddings are computed using a selected vision foundation model and can be indexed into a

production-grade k-nearest neighbors (KNN) engine with tuning for performance, latency, and resource constraints. Inference-A shows standard multimodal retrieval, where image and text embeddings are fused. Inference-B and Inference-C, proposed in our method, incorporate text rendering onto the image before generating the corresponding embeddings. Inference-B uses the text-rendered image alone, effectively retaining multimodal input within a single visual stream. Denoting the text-rendered image as \hat{i} and the image embedding function as $g(\cdot)$, retrieval reduces to finding the closest match via $S(g(\hat{i}_p), g(\hat{i}_p))$. Inference-C extends this one-encoder design by fusing the embedding of the text-rendered image with a separately encoded text embedding, thereby forming a hybrid multimodal representation. The similarity function is accordingly modified to $S(f(\hat{i_q}, t_q), f(\hat{i_p}, t_p))$. Note that text rendering is applied only during embedding generation and does not alter or replace the original images, thus avoiding any aesthetic or user-facing impact.

3.3 Typographic Factors

Typographic factors can impact how text appears in images [5, 7] and consequently alter the effectiveness of typographic attacks. Inspired by prior studies [5, 7], we investigate how these factors impact product retrieval. Specifically, we examine three dimensions: font size, font color, and spatial positioning of the rendered text, as illustrated in Figure 3. In e-commerce applications, sellers often upload images with arbitrary resolutions, and the available text (e.g. title, description, and/or item specifics) is typically longer than those used in adversarial attacks. Using absolute font size in such settings may result in text rendering which does not fit on the image. To address this, we first determine the maximum font size which fits the full rendered text within the image, and define the font size

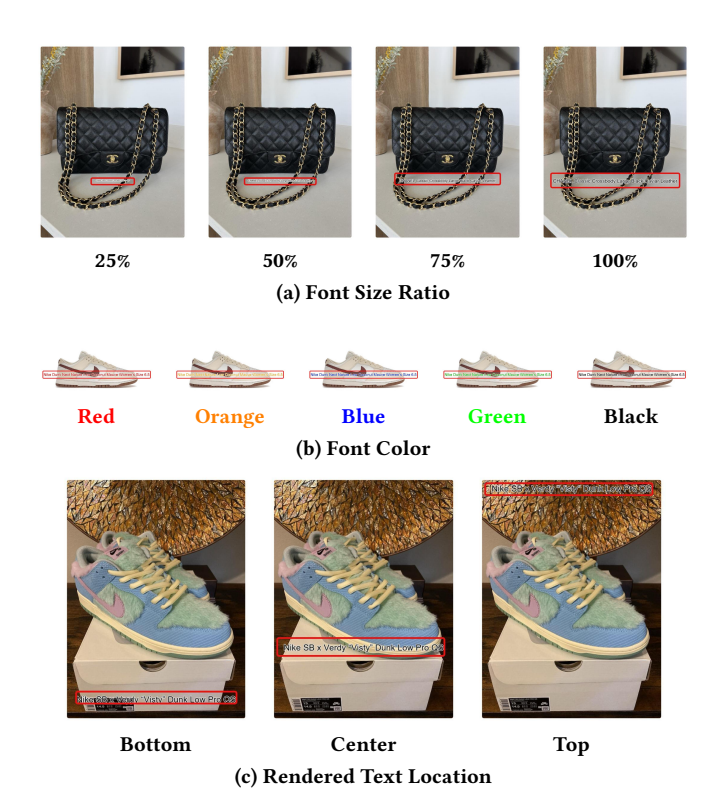


Figure 3: Illustration of typographic factors across the datasets used in our experiments: (a) Font Size Ratio, (b) Font Color, and (c) Rendered Text Location. Rendered text regions are highlighted with red boxes.

ratio as the percentage of the experimental font size relative to the maximum. This enables systematic analysis of how varying font size impacts retrieval performance.

To ensure the rendered text remains legible across a variety of inputs without any loss of key information, we implement a simple, computationally lightweight adaptive rendering algorithm, **GetMaxFontSize()**, that computes the maximum font size for a given text and renders it on the image using the ImageDraw module from PIL [9]. The pseudo-code for this text rendering procedure is provided in Algorithm 1. We further conduct an evaluation of the design factors to assess robustness and identify optimal configurations, with detailed analysis provided in Section 4.3.

4 Experiments

4.1 Datasets and Metrics

Table 1: Statistics of datasets used in the experiments.

| Dataset | Query # | Product # |
|---------------|---------|-----------|
| Sneakers | 1,986 | 139,567 |
| Handbags | 2,000 | 48,075 |
| Trading Cards | 1,127 | 400,683 |

Algorithm 1 Render Scaled Centered Text on an Image

```
Require: image I of width W and height H, text to render T
Ensure: Draw text T centered on the image I
  1: function GetMaxFontSize(I, T)
          W, H = size(I)
 2:
          s_{\text{max}}, s_{\text{min}}, w_{\text{max}} \leftarrow \lfloor W/6 \rfloor, 1, 0.9 \cdot W
 3:
 4:
          while s_{\min} < s_{\max} do
  5:
               s_{\text{mid}} \leftarrow \lfloor (s_{\text{min}} + s_{\text{max}} + 1)/2 \rfloor
               Load font with size s_{mid}
  6:
               Measure text width w<sub>mid</sub>
 7:
               if w_{\text{mid}} \le w_{\text{max}} then
 8:
                     s_{\min} \leftarrow s_{\min}
  9.
               else
10:
                     s_{\text{max}} \leftarrow s_{\text{mid}} - 1
11:
               end if
12:
          end while
13:
          return s_{\min}
14:
15: end function
16: function RenderText(I, T, x, y, c)
17:
          s \leftarrow \text{GetMaxFontSize}(I, T)
          Draw text T at location (x, y) with font-size s and font color
19: end function
```

We evaluate our method on three proprietary datasets from a major e-commerce platform, covering sneakers, handbags, and NBA trading cards. Dataset statistics are presented in Table 1. Each query has a single human-annotated ground-truth match.

NBA trading cards typically contain rich visual text (e.g., player and team names), while sneaker and handbag images often contain minimal text. This variation enables a controlled evaluation of how overlaying product metadata text affects multimodal retrieval performance. We report accuracy at rank k, Acc@k, defined as the proportion of queries for which the correct product is retrieved in the top k. We use Acc@1 and Acc@3 in our analysis.

Table 2: Overview of candidate models and their specifications.

| Collection | Model | Image Enc. | Text Enc. | |
|---------------|---------------------------------|------------|-----------|--|
| OpenAI | CLIP-L/14 | ✓ | ✓ | |
| PE | PE-Core-L14-336 | ✓ | ✓ | |
| SigLIP | SigLIP-SO400M/384 | ✓ | ✓ | |
| SigLIP 2 | SigLIP2-SO400M/384 | ✓ | ✓ | |
| Meta (DINOv2) | DINOv2-Large | ✓ | - | |
| Meta (DINOv3) | DINOv3-vitl16-pretrain-lvd1689m | ✓ | - | |

Due to the maximum token length constraints of the text encoders in most pretrained models, we employ an LLM to summarize all available item information including titles, descriptions, and attribute lists into a title-length text whenever the full text input is too long for the text encoder. This pre-processing step ensures that the most salient product information is preserved while maintaining compatibility with text encoders. In addition, this design choice simplifies implementation, reduces the risk of truncation errors, and provides a consistent textual representation that can be seamlessly integrated into the proposed retrieval enhancement method.

4.2 Main Results

We evaluate our enhancement method on five state-of-the-art vision foundation models across three product categories. CLIP [20], Perception Encoder (PE) [2], SigLIP [30], and SigLIP 2 [23] are dual-encoder models trained with contrastive learning to align image-text pairs in a shared embedding space. These models support zero-shot multimodal retrieval without requiring explicit labels or fine-grained annotations. SigLIP 2 extends the SigLIP design with self-distillation and masked prediction. We also include the DINO family (DINOV2 [17], DINOV3 [22]), a vision-only model trained with self-supervised learning to assess whether our method benefits models trained without textual supervision. Since all CLIP-like models evaluated in this study are limited to a small number of input text tokens, we use our generated title based on existing title, description, and attribute values.

As shown in Table 3, all candidate models are tested with raw and title-rendered image inputs. The rendered input is generated by applying Algorithm 1 with default factors, which overlays the title text onto the image. For multimodal retrieval, we evaluate two commonly used fusion strategies: *Sum* and *Concat*, resulting in six configurations per model. While other fusion strategies exist, identifying the optimal fusion method is beyond the scope of this work. All experiments are zero-shot with no fine-tuning to ensure a fair comparison. Model details are provided in Table 2.

From Table 3, we observe that across all three product categories, the highest performance metrics are generally obtained when models use title-rendered images, for both Acc@1 and Acc@3. This suggests that the proposed method consistently enhances product retrieval performance across all base models. Notably, SigLIP benefits the most, with an average improvement of 3.11 points in Acc@1 and 1.79 points in Acc@3 compared to the second-best configuration. This is particularly striking given that SigLIP already serves as the strongest baseline, indicating that the proposed enhancement can further improve even top-performing architectures. The Perception Encoder (PE) also demonstrates strong performance, showing comparable gains of 3.00 points in Acc@1 and 1.21 points in Acc@3, underscoring the general effectiveness of the proposed approach. Similar performance improvements are observed for the CLIP model as well.

SigLIP 2 exhibits some intriguing behavior in our experiments. When using raw images as input, multimodal retrieval with fused embeddings underperforms image-only retrieval in both the handbags and trading cards categories, whereas in the sneakers category, multimodal retrieval still provides a notable performance gain. Unlike CLIP, PE, and SigLIP, SigLIP 2 achieves its best results with title-rendered image-only retrieval. In particular, this configuration outperforms the second-best configuration by 8.21 points in Acc@1 and 3.69 points in Acc@3, suggesting that using a single image encoder on title-rendered inputs can serve as an effective alternative for multimodal retrieval when using SigLIP 2. One possible explanation is that the introduction of self-distillation and masked prediction in SigLIP 2's training may alter the alignment dynamics between image and text modalities in the joint embedding space learned during contrastive pretraining. However, we do not have definitive evidence to support this hypothesis, and further investigation is warranted.

From the empirical results in Table 3, we observe that the *Sum* fusion strategy consistently outperforms *Concat* across all models in the CLIP family. Furthermore, in all three categories, the proposed method using title-rendered images yields higher retrieval performance than raw image retrieval. It is also worth noting that the performance gains observed with DINOv2 and DINOv3 are less significant compared to the contrastive learning-based models, likely due to the lack of multimodal pretraining in its architecture.

4.3 Typographic Factors Matter

In this section, we study the impact of different typographic factors on product retrieval performance enhancement. For the three factors under study, we constrain font size ratio to {25%, 50%, 75%, 100%}, font colors to {red, blue, green, orange, black} and rendering locations to {top, middle, bottom}, ensuring generality and consistency in our evaluation. As observed in Section 4.2, models from the CLIP family benefit the most from the proposed enhancement method. Accordingly, in this study of typographic factors, we focus on four CLIP-family models: SigLIP, SigLIP 2, PE, and CLIP, and evaluate each on the Handbags and Sneakers datasets across all possible values of each factor.

Figure 4 presents Acc@1 and Acc@3 results across three typographic factors (Font Size Ratio, Font Color, and Rendered Text Location) for four models. Due to limited space, sneakers results can be found in Figure 6 in the Appendix. Each row corresponds to a distinct factor, while columns (from left to right) report Acc@1 and Acc@3 under inference settings B and C, respectively. As shown in Figure 4a, there is a positive correlation between the visibility of rendered text and the retrieval accuracy. A similar observation was made in [5, 7]. Notably, for strong models such as SigLIP, the performance gap can reach up to 15 absolute points in the Inference B Mode (rendered image only). However, the substantially smaller accuracy gap between smaller font size and maximum font size in Inference C (image + text) suggests that this factor becomes far less influential once fused embeddings are employed. We speculate that the reduced boost from smaller font rendering is partially compensated by the contribution of the text embeddings. For both font color and rendered text location, most models exhibit no substantial performance differences across different values. Nonetheless, the CLIP model shows a clear preference for text rendered at the center, compared to top or bottom placements.

This study demonstrates that typographic factors, particularly font size, have a substantial impact on the effectiveness of the proposed enhancement method. Based on these findings, we recommend setting the default configuration in real-world applications to {Max font size, Black, Center}.

4.4 Case Study

Figure 1 presents an example featuring the Nike SB Dunk Pro Verdy Visty sneakers, which serves as the focus of this case study. Due to space constraints, we highlight results using the SigLIP model in this case study, which was selected based on its strong performance demonstrated in the previous section. We conducted two types of multimodal retrieval: (1) raw image combined with the title, and (2) the title rendered on the image combined with the same title as a separate input. Figure 5 shows the top 3 retrieved products for each

| Model | Image | Text | Fusion | Sneakers | | Handbags | | Trading Cards | |
|---------------|----------|-------|--------|----------|--------|----------|--------|---------------|--------|
| | | | | Acc@1 | Acc@3 | Acc@1 | Acc@3 | Acc@1 | Acc@3 |
| CLIP [20] | Raw | - | _ | 0.2185 | 0.2578 | 0.0450 | 0.0600 | 0.1624 | 0.2396 |
| | Raw | Title | Sum | 0.7014 | 0.7578 | 0.2285 | 0.2900 | 0.5439 | 0.7276 |
| | Raw | Title | Concat | 0.7004 | 0.7563 | 0.2355 | 0.2950 | 0.5306 | 0.6983 |
| | Rendered | _ | _ | 0.2790 | 0.3132 | 0.0810 | 0.1195 | 0.2094 | 0.3132 |
| | Rendered | Title | Sum | 0.7175 | 0.7679 | 0.2515 | 0.3130 | 0.5972 | 0.7737 |
| | Rendered | Title | Concat | 0.6883 | 0.7356 | 0.2450 | 0.3045 | 0.5626 | 0.7329 |
| | Raw | _ | _ | 0.5272 | 0.5992 | 0.0870 | 0.1425 | 0.4694 | 0.6850 |
| | Raw | Title | Sum | 0.8036 | 0.8505 | 0.2435 | 0.3275 | 0.8128 | 0.9388 |
| PE [2] | Raw | Title | Concat | 0.7925 | 0.8439 | 0.2545 | 0.3260 | 0.7720 | 0.9228 |
| FE [2] | Rendered | _ | _ | 0.7180 | 0.7618 | 0.1820 | 0.2600 | 0.5484 | 0.7915 |
| | Rendered | Title | Sum | 0.8127 | 0.8484 | 0.2955 | 0.3635 | 0.8421 | 0.9414 |
| | Rendered | Title | Concat | 0.8006 | 0.8374 | 0.2940 | 0.3645 | 0.8030 | 0.9272 |
| | Raw | _ | _ | 0.4547 | 0.5176 | 0.1245 | 0.2125 | 0.5590 | 0.7870 |
| | Raw | Title | Sum | 0.7684 | 0.8278 | 0.3035 | 0.3685 | 0.8350 | 0.9379 |
| Cial ID [20] | Raw | Title | Concat | 0.7523 | 0.8087 | 0.3075 | 0.3720 | 0.8163 | 0.9104 |
| SigLIP [30] | Rendered | _ | _ | 0.7523 | 0.7895 | 0.2910 | 0.3615 | 0.6761 | 0.8634 |
| | Rendered | Title | Sum | 0.8006 | 0.8429 | 0.3320 | 0.3930 | 0.8616 | 0.9335 |
| | Rendered | Title | Concat | 0.7835 | 0.8212 | 0.3295 | 0.3895 | 0.8270 | 0.9148 |
| SigLIP 2 [23] | Raw | - | _ | 0.4300 | 0.5000 | 0.1250 | 0.2075 | 0.4747 | 0.7249 |
| | Raw | Title | Sum | 0.6440 | 0.7407 | 0.0755 | 0.1240 | 0.2209 | 0.3372 |
| | Raw | Title | Concat | 0.6375 | 0.7402 | 0.0800 | 0.1300 | 0.2227 | 0.3407 |
| | Rendered | _ | _ | 0.6636 | 0.7105 | 0.2390 | 0.3200 | 0.5954 | 0.7533 |
| | Rendered | Title | Sum | 0.4607 | 0.5705 | 0.1275 | 0.1790 | 0.2422 | 0.3274 |
| | Rendered | Title | Concat | 0.4673 | 0.5801 | 0.1330 | 0.1835 | 0.2520 | 0.3319 |
| DINOv2 [17] | Raw | _ | | 0.0358 | 0.0468 | 0.0645 | 0.1035 | 0.2760 | 0.4153 |
| | Rendered | - | - | 0.0352 | 0.0443 | 0.0695 | 0.1120 | 0.2964 | 0.4357 |
| DINOv3 [22] | Raw | _ | _ | 0.1616 | 0.1868 | 0.089 | 0.145 | 0.3975 | 0.5936 |
| | Rendered | _ | _ | 0.1752 | 0.2039 | 0.075 | 0.127 | 0.4099 | 0.6087 |

Table 3: Performance of candidate models across different image input types, retrieval modalities, and fusion strategies on three product categories. The highest metric value for each model and product category is highlighted in bold.

setting. As shown, the proposed approach (bottom row), which uses the title-rendered image, successfully retrieves the correct product as the top-1 result. In contrast, the correct match is entirely missing from the top row, despite the visual similarity of other retrieved items. We have observed similar improvements using the proposed method across other samples and candidate models. Due to space constraints, additional qualitative examples across different categories are provided in the Appendix (Figures 7–13).

5 Conclusions and Future Work

In this paper, we introduce a novel approach for improving multimodal product retrieval by reversing the logic of typographic attacks via vision-text compression. In contrast to prior work that treats rendered text as adversarial noise, we enhance product retrieval by overlaying relevant textual information directly onto images. This improves image-text alignment in vision-language

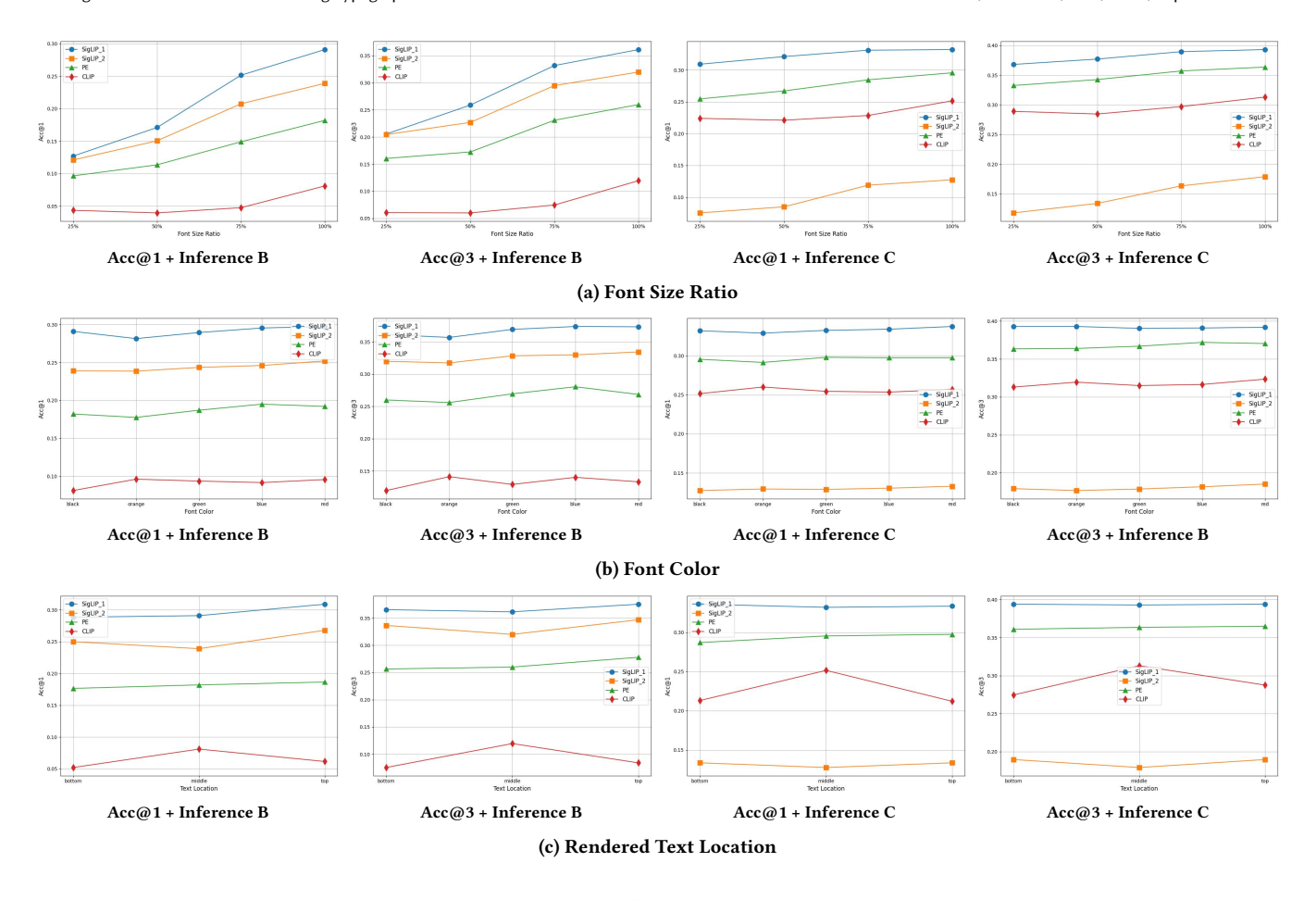


Figure 4: Acc@1 and Acc@3 across three typographic factors (Font Size Ratio, Font Color, and Rendered Text Location) for four models (SigLIP, SigLIP 2, PE, and CLIP) on the Handbags dataset. Rows correspond to the three typographic factors, while columns report Acc@1 and Acc@3 under inference settings B and C, respectively.

models without requiring architectural changes or additional model training. Across zero-shot evaluations on proprietary e-commerce datasets and state-of-the-art encoders, our approach consistently improves retrieval performance in both unimodal and multimodal settings. We observe gains in Acc@1 and Acc@3 across all contrastive learning-based models in our experiment, including the widely used CLIP and SigLIP. Visualizations of attention sensitivity maps and qualitative case studies further support the effectiveness of our approach. Given its minimal latency and resource overhead, the proposed method is well-suited for deployment in real-world multimodal product retrieval systems.

Our study primarily focuses on enhancing multimodal product retrieval in a zero-shot setting using pretrained vision-language models. While preliminary findings suggest that the proposed method may also be beneficial during model fine-tuning and pretraining, we leave a systematic assessment of its generalizability across training paradigms to future work.

References

 Hiroki Azuma and Yusuke Matsui. 2023. Defense-Prefix for Preventing Typographic Attacks on CLIP. https://arxiv.org/abs/2304.04512

- [2] Daniel Bolya, Po-Yao Huang, Peize Sun, Jang Hyun Cho, Andrea Madotto, Chen Wei, Tengyu Ma, Jiale Zhi, Jathushan Rajasegaran, Hanoona Rasheed, Junke Wang, Marco Monteiro, Hu Xu, Shiyu Dong, Nikhila Ravi, Daniel Li, Piotr Dollár, and Christoph Feichtenhofer. 2025. Perception Encoder: The best visual embeddings are not at the output of the network. arXiv preprint (2025). https://arxiv.org/abs/2504.13181
- [3] Walid Bousselham, Angie Boggust, Sofian Chaybouti, Hendrik Strobelt, and Hilde Kuehne. 2025. LeGrad: An Explainability Method for Vision Transformers via Feature Formation Sensitivity. arXiv:2404.03214 [cs.CV] https://arxiv.org/abs/ 2404.03214
- [4] Liangliang Cao, Bowen Zhang, Chen Chen, Yinfei Yang, Xianzhi Du, Wencong Zhang, Zhiyun Lu, and Yantao Zheng. 2023. Less is More: Removing Text-regions Improves CLIP Training Efficiency and Robustness. arXiv:2305.05095 [cs.CV] https://arxiv.org/abs/2305.05095
- [5] Hao Cheng, Erjia Xiao, Jindong Gu, Le Yang, Jinhao Duan, Jize Zhang, Jiahang Cao, Kaidi Xu, and Renjing Xu. 2024. Unveiling Typographic Deceptions: Insights of the Typographic Vulnerability in Large Vision-Language Model. arXiv:2402.19150 [cs.CV] https://arxiv.org/abs/2402.19150
- [6] Hao Cheng, Erjia Xiao, Yichi Wang, Kaidi Xu, Mengshu Sun, Jindong Gu, and Renjing Xu. 2025. Exploring Typographic Visual Prompts Injection Threats in Cross-Modality Generation Models. arXiv:2503.11519 [cs.CV] https://arxiv.org/ abs/2503.11519
- [7] Hao Cheng, Erjia Xiao, Jiayan Yang, Jiahang Cao, Qiang Zhang, Jize Zhang, Kaidi Xu, Jindong Gu, and Renjing Xu. 2025. Not Just Text: Uncovering Vision Modality Typographic Threats in Image Generation Models. arXiv:2412.05538 [cs.CV] https://arxiv.org/abs/2412.05538
- [8] Jiale Cheng, Yusen Liu, Xinyu Zhang, Yulin Fei, Wenyi Hong, Ruiliang Lyu, Weihan Wang, Zhe Su, Xiaotao Gu, Xiao Liu, Yushi Bai, Jie Tang, Hongning

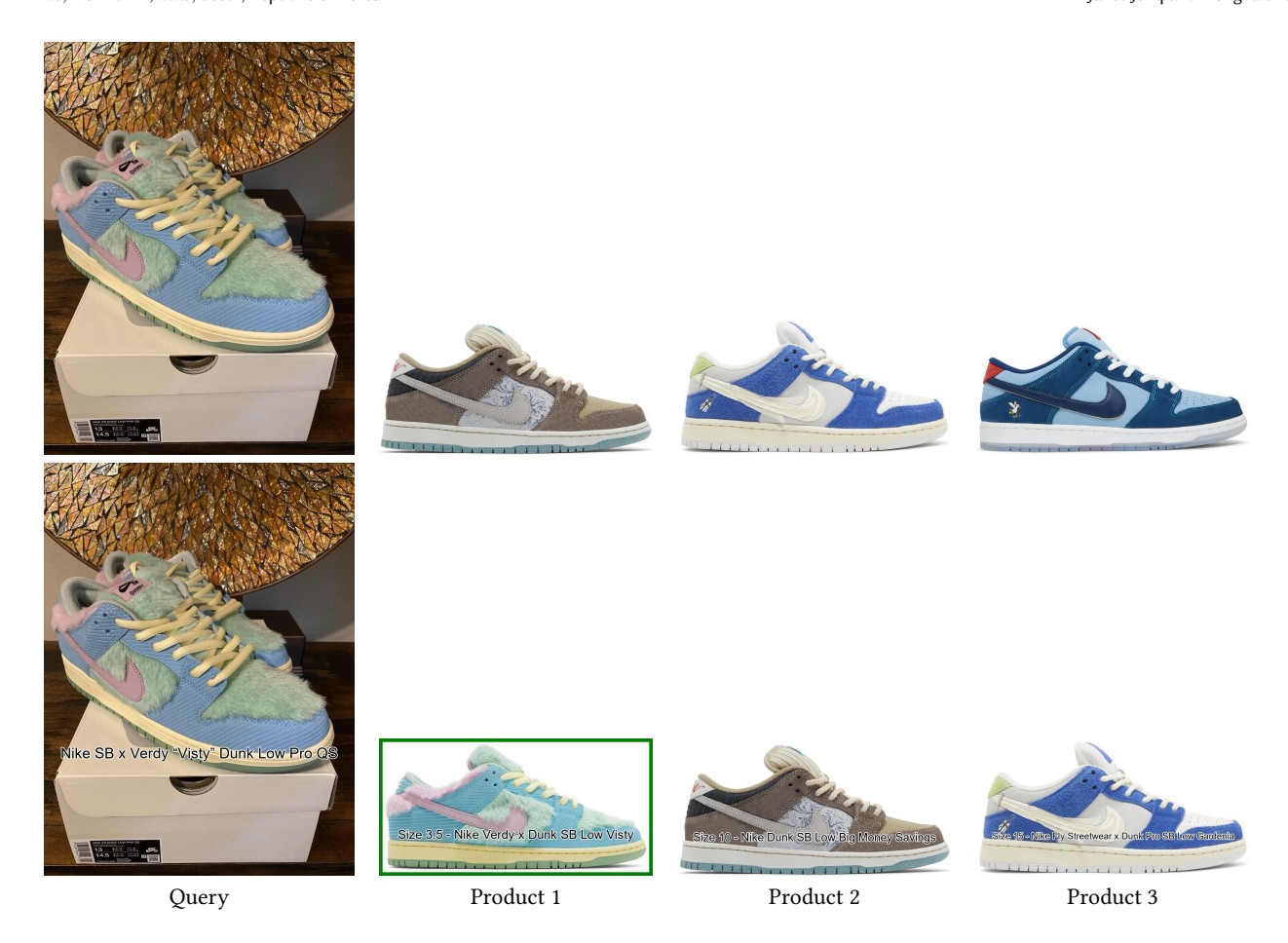


Figure 5: Example from the sneakers category showing the query and retrieved products under raw (top row) and title-rendered (bottom row) conditions. The top row shows the original query image and three retrieved product images. The bottom row shows the corresponding images with listing titles rendered using our proposed method. The correct product match is highlighted with a green box.

- Wang, and Minlie Huang. 2025. Glyph: Scaling Context Windows via Visual-Text Compression. arXiv:2510.17800 [cs.CV] https://arxiv.org/abs/2510.17800
- [9] Alex Clark et al. 2025. Pillow (PIL Fork) Documentation. https://buildmedia.readthedocs.org/media/pdf/pillow/latest/pillow.pdf
- [10] Gabriel Goh, Nick Cammarata †, Chelsea Voss †, Shan Carter, Michael Petrov, Ludwig Schubert, Alec Radford, and Chris Olah. 2021. Multimodal Neurons in Artificial Neural Networks. *Distill* (2021). doi:10.23915/distill.00030 https://distill.pub/2021/multimodal-neurons.
- [11] Jinyuan Jia, Yupei Liu, and Neil Zhenqiang Gong. 2022. BadEncoder: Backdoor Attacks to Pre-trained Encoders in Self-Supervised Learning. In Proceedings - 43rd IEEE Symposium on Security and Privacy, SP 2022 (Proceedings - IEEE Symposium on Security and Privacy). 2043–2059.
- [12] Yoann Lemesle, Masataka Sawayama, Guillermo Valle-Perez, Maxime Adolphe, Hélène Sauzéon, and Pierre-Yves Oudeyer. 2022. Language-biased image classification: evaluation based on semantic representations. arXiv:2201.11014 [cs.CV] https://arxiv.org/abs/2201.11014
- [13] Yiqi Lin, Conghui He, Alex Jinpeng Wang, Bin Wang, Weijia Li, and Mike Zheng Shou. 2025. Parrot Captions Teach CLIP to Spot Text. In Computer Vision – ECCV 2024, Aleš Leonardis, Elisa Ricci, Stefan Roth, Olga Russakovsky, Torsten Sattler, and Gül Varol (Eds.). Springer Nature Switzerland, Cham, 368–385.
- [14] Dong Liu and Esther Lopez Ramos. 2025. Multimodal Semantic Retrieval for Product Search. In Companion Proceedings of the ACM on Web Conference 2025 (Sydney NSW, Australia) (WWW '25). Association for Computing Machinery, New York, NY, USA, 2170–2175. https://doi.org/10.1145/3701716.3717567
- [15] Pratyush Maini, Sachin Goyal, Zachary C. Lipton, J. Zico Kolter, and Aditi Raghunathan. 2024. T-MARS: Improving Visual Representations by Circumventing Text Feature Learning. arXiv:2307.03132 [cs.CV] https://arxiv.org/abs/2307.03132

- [16] David A. Noever and Samantha E. Miller Noever. 2021. Reading Isn't Believing: Adversarial Attacks On Multi-Modal Neurons. arXiv:2103.10480 [cs.LG] https://arxiv.org/abs/2103.10480
- [17] Maxime Oquab, Timothée Darcet, Théo Moutakanni, Huy Q. Vo, Marc Szafraniec, Vasil Khalidov, Pierre Fernandez, Daniel Haziza, Francisco Massa, Alaaeldin El-Nouby, Mahmoud Assran, Nicolas Ballas, Wojciech Galuba, Russ Howes, Po-Yao (Bernie) Huang, Shang-Wen Li, Ishan Misra, Michael G. Rabbat, Vasu Sharma, Gabriel Synnaeve, Huijiao Xu, Hervé Jégou, Julien Mairal, Patrick Labatut, Armand Joulin, and Piotr Bojanowski. 2023. DINOv2: Learning Robust Visual Features without Supervision. ArXiv abs/2304.07193 (2023). https://api.semanticscholar.org/CorpusID:258170077
- [18] Maan Qraitem, Nazia Tasnim, Piotr Teterwak, Kate Saenko, and Bryan A. Plummer. 2025. Vision-LLMs Can Fool Themselves with Self-Generated Typographic Attacks. arXiv:2402.00626 [cs.CV] https://arxiv.org/abs/2402.00626
- [19] Maan Qraitem, Piotr Teterwak, Kate Saenko, and Bryan A. Plummer. 2025. Web Artifact Attacks Disrupt Vision Language Models. arXiv:2503.13652 [cs.CV] https://arxiv.org/abs/2503.13652
- [20] Alec Radford, Jong Wook Kim, Chris Hallacy, Aditya Ramesh, Gabriel Goh, Sandhini Agarwal, Girish Sastry, Amanda Askell, Pamela Mishkin, Jack Clark, Gretchen Krueger, and Ilya Sutskever. 2021. Learning Transferable Visual Models From Natural Language Supervision. In Proceedings of the 38th International Conference on Machine Learning (Proceedings of Machine Learning Research, Vol. 139), Marina Meila and Tong Zhang (Eds.). PMLR, 8748–8763. https://proceedings.mlr.press/v139/radford21a.html
- [21] Zhaochun Ren, Xiangnan He, Dawei Yin, and Maarten de Rijke. 2018. Information Discovery in E-commerce: Half-day SIGIR 2018 Tutorial (SIGIR '18). Association for Computing Machinery, New York, NY, USA, 1379–1382. https://doi.org/10.

1145/3209978 3210185

- [22] Oriane Siméoni, Huy V. Vo, Maximilian Seitzer, Federico Baldassarre, Maxime Oquab, Cijo Jose, Vasil Khalidov, Marc Szafraniec, Seungeun Yi, Michaël Ramamonjisoa, Francisco Massa, Daniel Haziza, Luca Wehrstedt, Jianyuan Wang, Timothée Darcet, Théo Moutakanni, Leonel Sentana, Claire Roberts, Anfrea Vedaldi, Jamie Tolan, John Brandt, Camille Couprie, Julien Mairal, Hervé Jégou, Patrick Labatut, and Piotr Bojanowski. 2025. DINOv3. arXiv:2508.10104 [cs.CV] https://arxiv.org/abs/2508.10104
- [23] Michael Tschannen, Alexey Gritsenko, Xiao Wang, Muhammad Ferjad Naeem, Ibrahim Alabdulmohsin, Nikhil Parthasarathy, Talfan Evans, Lucas Beyer, Ye Xia, Basil Mustafa, Olivier Hénaff, Jeremiah Harmsen, Andreas Steiner, and Xiaohua Zhai. 2025. SigLIP 2: Multilingual Vision-Language Encoders with Improved Semantic Understanding, Localization, and Dense Features. arXiv:2502.14786 [cs.CV] https://arxiv.org/abs/2502.14786
- [24] Michael Tschannen, Basil Mustafa, and Neil Houlsby. 2023. CLIPPO: Imageand-Language Understanding From Pixels Only. In Proceedings of the IEEE/CVF Conference on Computer Vision and Pattern Recognition (CVPR). 11006–11017.
- [25] Sándor Tóth, Stephen Wilson, Alexia Tsoukara, Enric Moreu, Anton Masalovich, and Lars Roemheld. 2024. End-to-end multi-modal product matching in fashion e-commerce. arXiv:2403.11593 [cs.CV] https://arxiv.org/abs/2403.11593
- [26] Qizhou Wang, Yong Lin, Yongqiang Chen, Ludwig Schmidt, Bo Han, and Tong Zhang. 2024. A Sober Look at the Robustness of CLIPs to Spurious Features. In Advances in Neural Information Processing Systems, Vol. 37. 122484–122523.
- [27] Weizhi Wang, Khalil Mrini, Linjie Yang, Sateesh Kumar, Yu Tian, Xifeng Yan, and Heng Wang. 2024. Finetuned Multimodal Language Models Are High-Quality Image-Text Data Filters. arXiv:2403.02677 [cs.CV] https://arxiv.org/abs/2403.

- 02677
- [28] Haoran Wei, Yaofeng Sun, and Yukun Li. 2025. DeepSeek-OCR: Contexts Optical Compression. arXiv:2510.18234 [cs.CV] https://arxiv.org/abs/2510.18234
- [29] Licheng Yu, Jun Chen, Animesh Sinha, Mengjiao Wang, Yu Chen, Tamara L. Berg, and Ning Zhang. 2022. CommerceMN: Large-Scale Commerce MultiModal Representation Learning with Omni Retrieval. In Proceedings of the 28th ACM SIGKDD Conference on Knowledge Discovery and Data Mining (Washington DC, USA) (KDD '22). Association for Computing Machinery, New York, NY, USA, 4433–4442. https://doi.org/10.1145/3534678.3539151
- [30] Xiaohua Zhai, Basil Mustafa, Alexander Kolesnikov, and Lucas Beyer. 2023. Sigmoid Loss for Language Image Pre-Training. In Proceedings of the IEEE/CVF International Conference on Computer Vision (ICCV). 11975–11986.
- [31] Xiaoyang Zheng, Fuyu Lv, Zilong Wang, Qingwen Liu, and Xiaoyi Zeng. 2023. Delving into E-Commerce Product Retrieval with Vision-Language Pre-training. In Proceedings of the 46th International ACM SIGIR Conference on Research and Development in Information Retrieval (Taipei, Taiwan) (SIGIR '23). Association for Computing Machinery, New York, NY, USA, 3385–3389.
- [32] Xiaoyang Zheng, Zilong Wang, Sen Li, Ke Xu, Tao Zhuang, Qingwen Liu, and Xiaoyi Zeng. 2023. MAKE: Vision-Language Pre-training based Product Retrieval in Taobao Search. In Companion Proceedings of the ACM Web Conference 2023 (Austin, TX, USA) (WWW '23 Companion). Association for Computing Machinery, New York, NY, USA, 356–360. https://doi.org/10.1145/3543873.3584627

Appendix

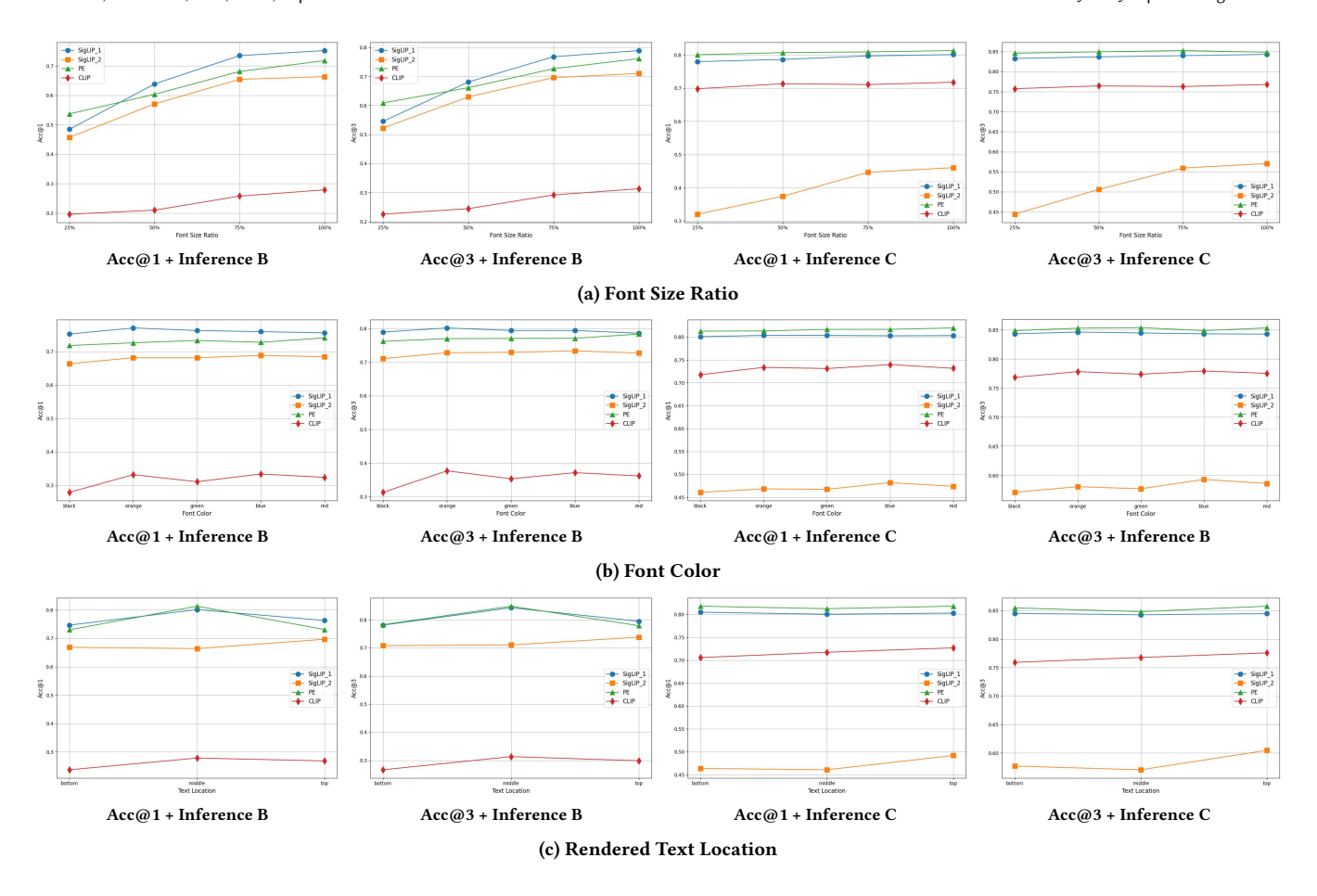


Figure 6: Acc@1 and Acc@3 results across three typographic factors (Font Size Ratio, Font Color, and Rendered Text Location) for four models (SigLIP, SigLIP 2, PE, and CLIP) on the Sneakers dataset. Rows correspond to the three typographic factors, while columns report Acc@1 and Acc@3 under inference settings B and C, respectively.



Figure 7: Example from the sneakers category showing the query and retrieved products under raw (top row) and title-rendered (bottom row) conditions. The top row shows the original query image and three retrieved product images. The bottom row shows the corresponding images with listing titles rendered using our proposed method. The correct product match is highlighted with a green box.

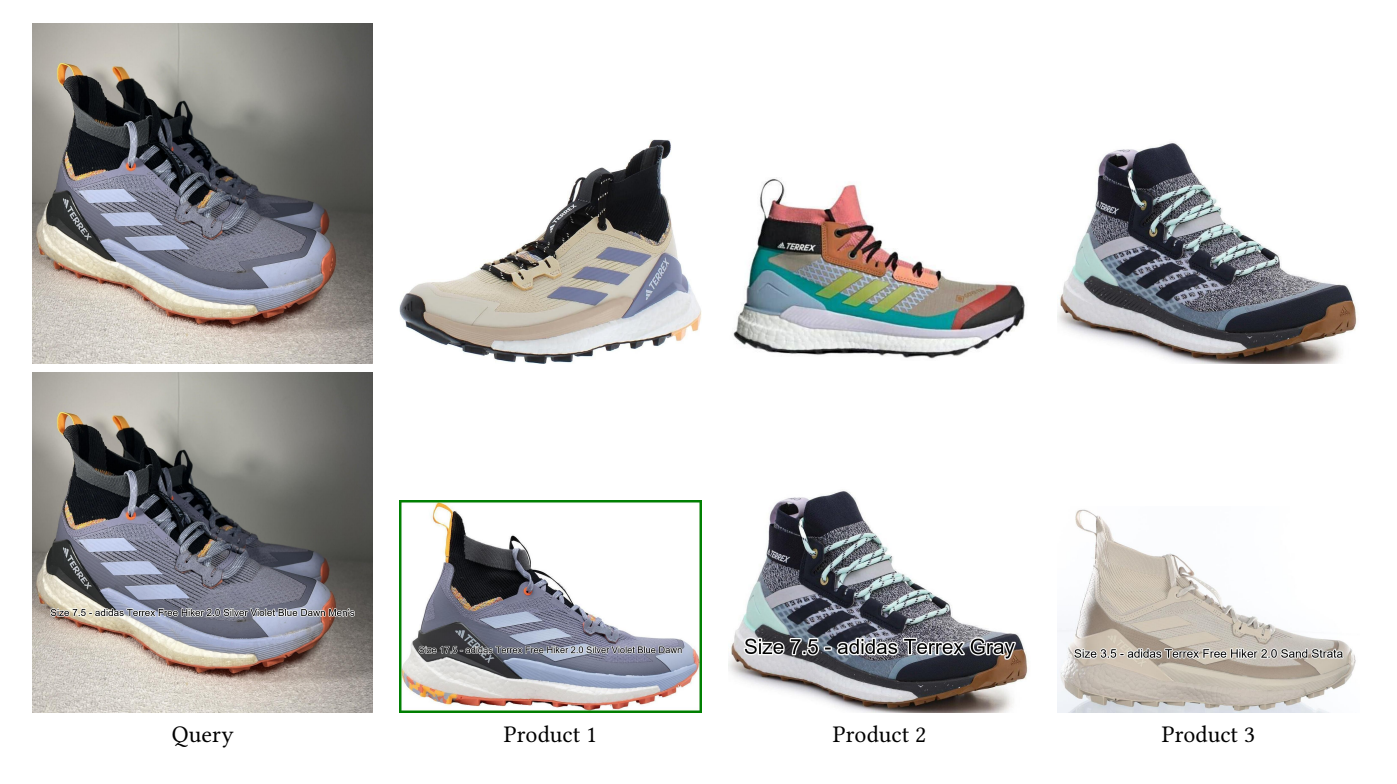


Figure 8: Example from the sneakers category showing the query and retrieved products under raw (top row) and title-rendered (bottom row) conditions. The top row shows the original query image and three retrieved product images. The bottom row shows the corresponding images with listing titles rendered using our proposed method. The correct product match is highlighted with a green box.



Figure 9: Example from the handbags category showing the query and retrieved products under raw (top row) and title-rendered (bottom row) conditions. The top row shows the original query image and three retrieved product images. The bottom row shows the corresponding images with listing titles rendered using our proposed method. The correct product match is highlighted with a green box.

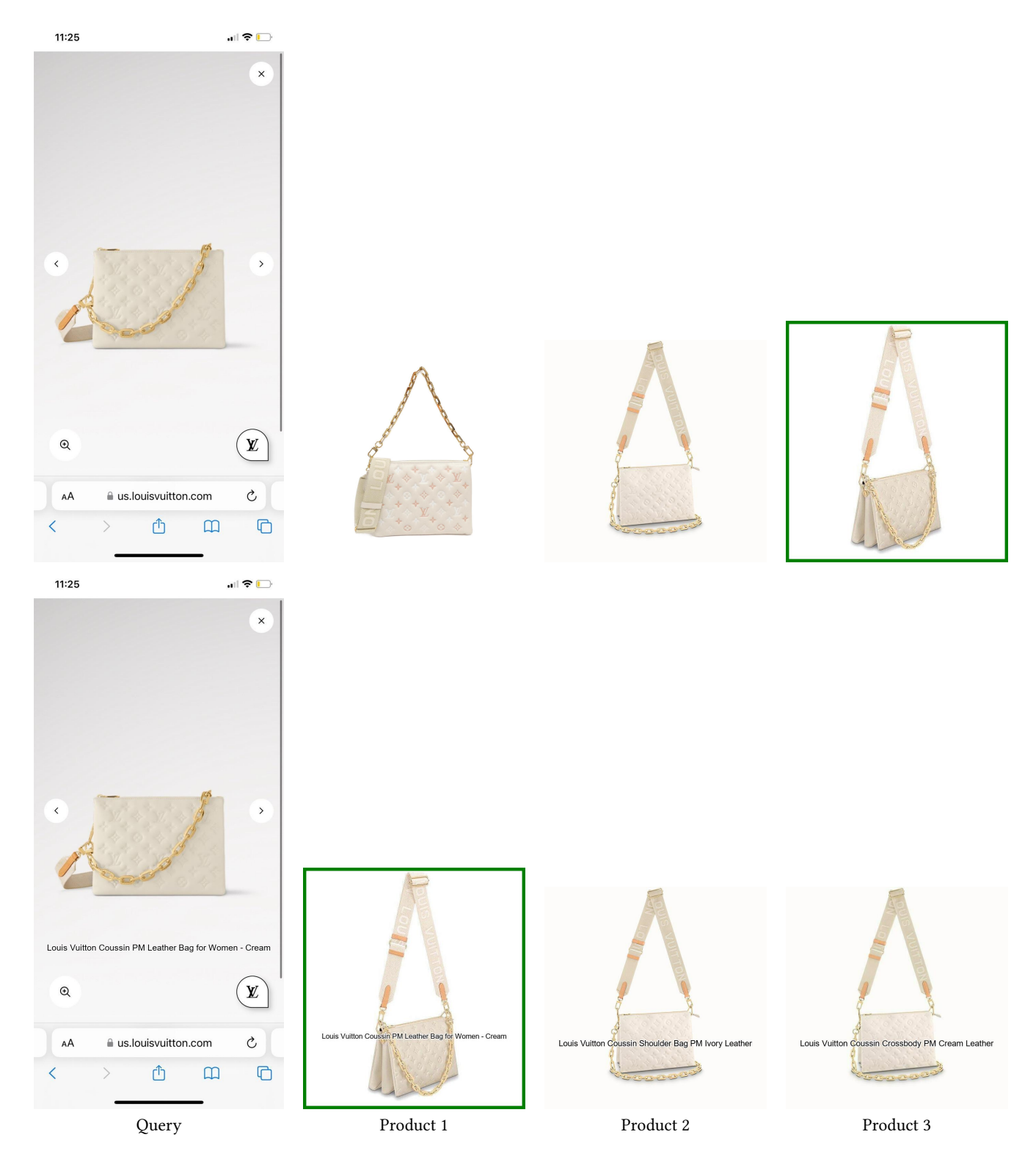


Figure 10: Example from the handbags category showing the query and retrieved products under raw (top row) and title-rendered (bottom row) conditions. The top row shows the original query image and three retrieved product images. The bottom row shows the corresponding images with listing titles rendered using our proposed method. The correct product match is highlighted with a green box.

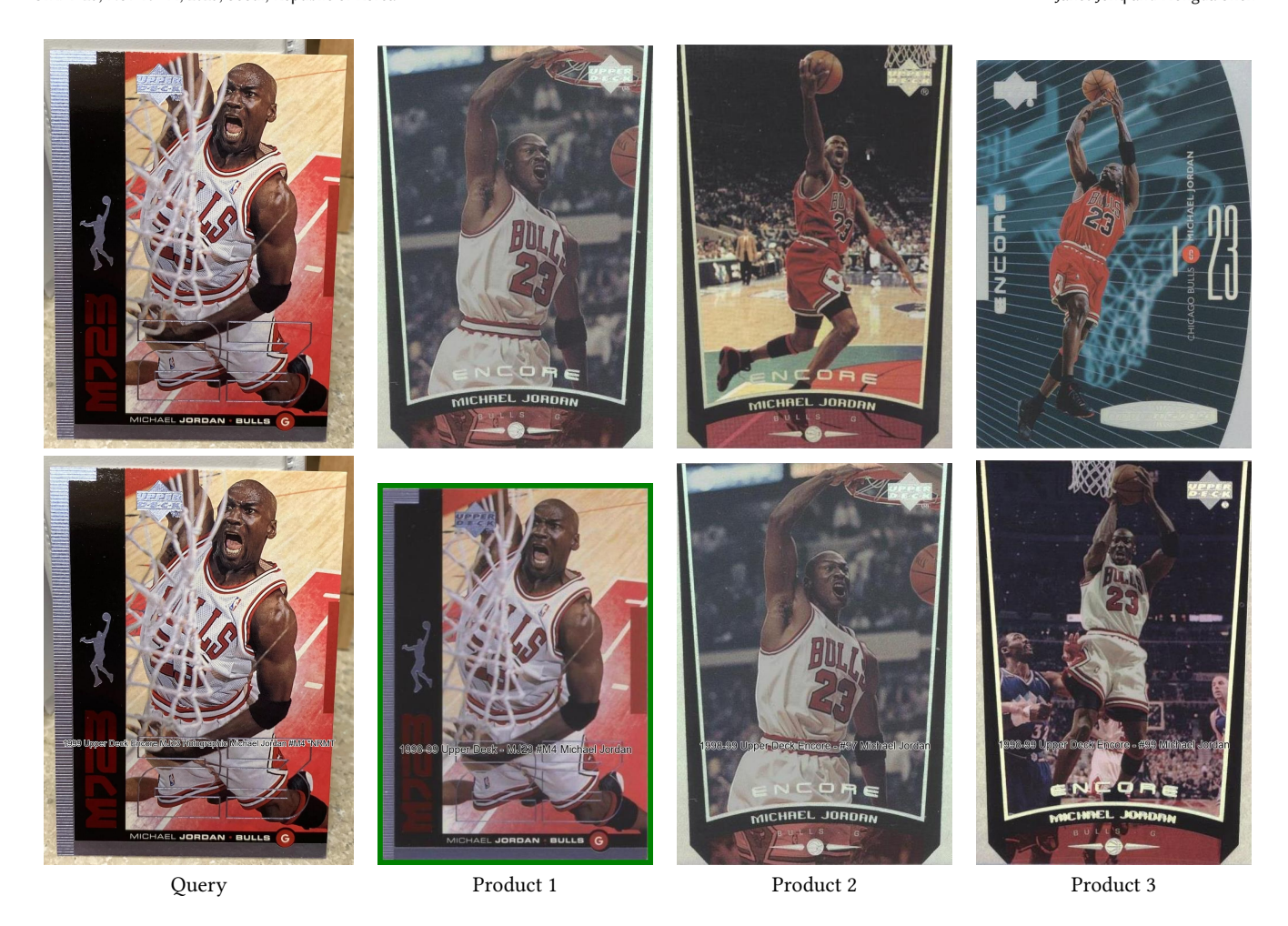


Figure 11: Example from the trading cards category showing the query and retrieved products under raw (top row) and title-rendered (bottom row) conditions. The top row shows the original query image and three retrieved product images. The bottom row shows the corresponding images with listing titles rendered using our proposed method. The correct product match is highlighted with a green box.



Figure 12: Example from the trading cards category showing the query and retrieved products under raw (top row) and title-rendered (bottom row) conditions. The top row shows the original query image and three retrieved product images. The bottom row shows the corresponding images with listing titles rendered using our proposed method. The correct product match is highlighted with a green box.

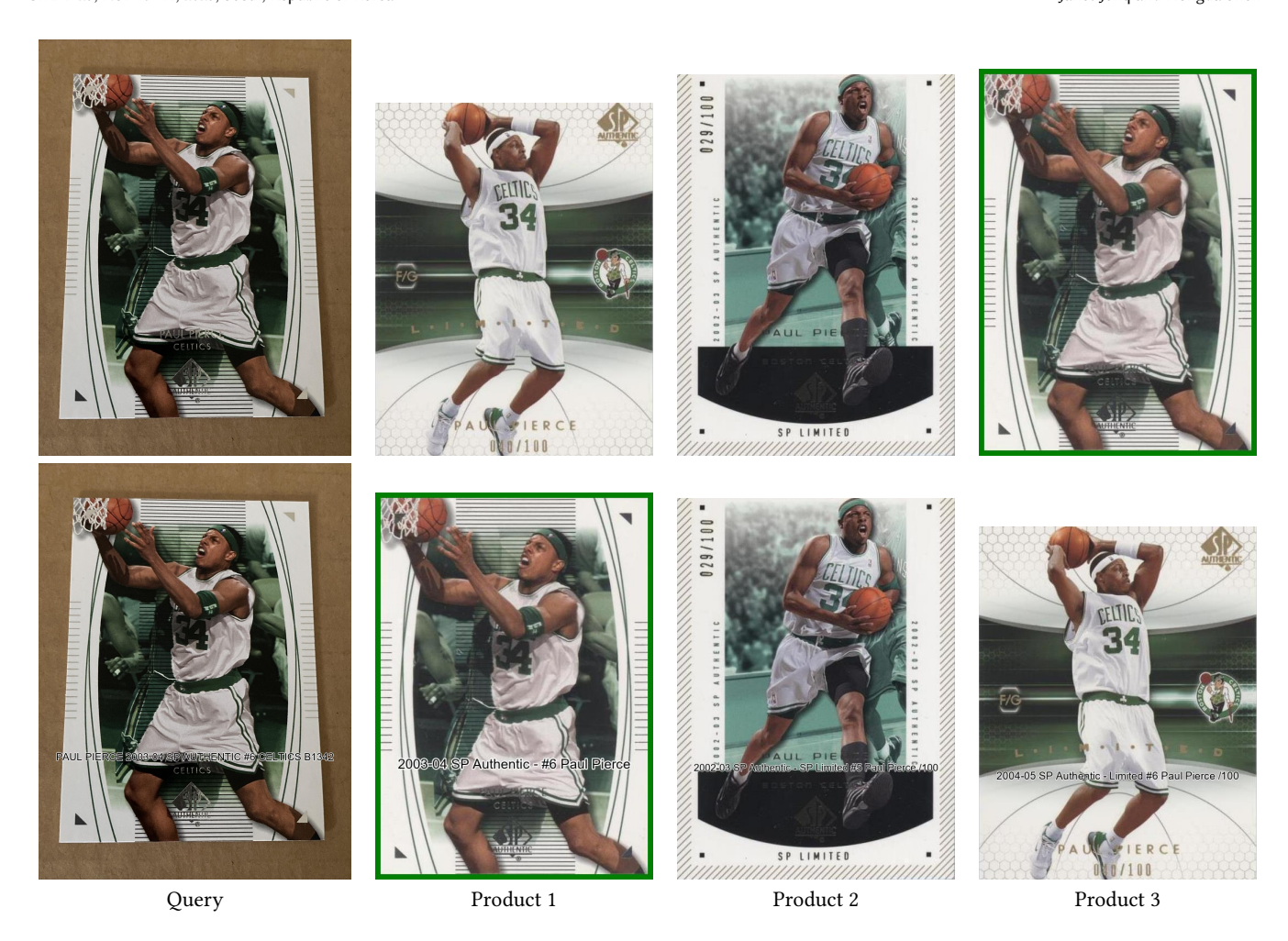


Figure 13: Example from the trading cards category showing the query and retrieved products under raw (top row) and title-rendered (bottom row) conditions. The top row shows the original query image and three retrieved product images. The bottom row shows the corresponding images with listing titles rendered using our proposed method. The correct product match is highlighted with a green box.